AGL61/80 regulates *BGAL9*, which participates in early somatic embryogenesis and increases longan resistance to heat stress

Yan Chen[1,2#], Xiangwei Ma[1,3#], Wentao Ma[1], Luzhen Xu[1], Chunwang Lai[1], Xueying Zhang[1], Qing Guan[1], Zihao Zhang[1], Yukun Chen[1], Zhongxiong Lai[1*] and Yuling Lin[1*]

[1] *Institute of Horticultural Biotechnology, Fujian Agriculture and Forestry University, Fuzhou 350002, Fujian, China*
[2] *Fujian Engineering Research Center for Characteristic Floriculture, Institute of Crop Sciences, Fujian Academy of Agricultural Sciences(Fujian Germplasm Resources Center), Fuzhou 350013, Fujian, China*
[3] *Guangxi Subtropical Crops Research Institute, Nanning 530010, Guangxi, China*
[#] These authors contributed equally: Yan Chen, Xiangwei Ma
[*] Corresponding authors, E-mail: laizx01@163.com; buliang84@163.com

Abstract

β-galactosidase (BGAL) is a glycosyl hydrolase that participates in cell wall modification, playing an essential role in plant growth, development and environmental stress adaptation. However, the function of *BGALs* in longan remains unclear. In this study, a total of 20 *BGAL* genes were identified from the longan (*Dimocarpus longan* Lour.) genome, which were distributed to eight chromosomes. Transcript profiles revealed that the majority of 11 detected *DlBGAL* genes were highly expressed in the embryogenic callus (EC) (four) and globular embryos (GE) (six), and responsive to heat stress. Combined with RNA-seq, ATAC-seq, and ChIP-seq results, most *DlBGAL* genes differentially expressed during early somatic embryogenesis (SE) were related with chromatin accessibility and high levels of H3K4me1. *DlBGAL9* was selected for further analysis. Dual-luciferase assays and transient transformation indicated that the transcription factor (TF) DlAGL61 and DlAGL80 might bind to the *DlBGAL9* promoters to activate *DlBGAL9* transcription. Overexpression of *DlBGAL9* and TF *DlAGL80* induces longan hairy roots *β*-GAL activity and thickening of cell walls. The expression levels of *DlBGAL9* and TF *DlAGL80* in longan hairy roots were significantly increased under heat stress, and ROS scavengers related genes were significantly upregulated in overexpressing *DlBGAL9* and TF *DlAGL80* hairy roots. This study proposes the significance of the regulatory network composed of *DlBGAL9* and TF *DlAGL80* in regulating the early longan SE and heat stress response.

Introduction

β-galactosidase (BGAL; EC 3.2.1.23) is one of the oldest ubiquitous enzymes and exists widely in higher plants. *BGAL* catalyzes the hydrolysis of polysaccharides, glycoproteins and terminal non-reducing *β*-D-galactosyl residues[1]. *BGALs* with this hydrolytic activity exist in the glycoside hydrolase (GH) family (GH1/2/3/35/42/50/59), and plants *BGAL* belongs to the GH35 family[2,3]. In plants, *BGALs* can be divided into two types based on their substrate specificities: Class I is an enzyme consisting of exo-*β*-(1-4)-galactanases that acts specifically on pectin *β*-(1-4)-D galactan. Class II have no hydrolytic activity against *β*-(1-4)-galactan and acts on the *β*-(1-3) and *β*-(1-6)-galactosyl linkages of arabinogalactan proteins[4]. *BGALs* participate in a variety of biological processes, particularly playing a privotal role in seed germination, cell-growth and fruit maturation[5,6].

Multigene family of *BGALs* has been identified in a variety of plant species, including Arabidopsis[7], rice[8], tomato[9], and sweet potato[10]. Plant *BGALs* were widely involved in the modification of cell wall structure and intercellular connections[11,12]. In Arabidopsis, *BGALs* may participate in cell wall metabolism in many processes[13]. *AtBGAL1/2/3/4* were involved in growth, *AtBGAL12* was involved in differentiation and *AtBGAL5* was involved in hairy root development. Moreover, all *AtBGAL*

transcripts occur during the initial stage of development[14]. In tomato, 17 putative *BGAL* encoding isoenzymes have been identified, which have different physiological functions and subcellular localization. At least seven of these genes contributed to the total *β*-GAL enzyme activity, and the transcription of corresponding genes differed significantly between early and late ripening of tomato fruits[15]. In chickpeas, the expression of *CanBGal-5* was associated with growth and maturation stages with high cell division rate, while *CanBGal-1* and *CanBGal-4* were closely associated with late epicotyl growth[16]. Moreover, the *BGAL* family was also regulated by biological and abiotic stresses[17]. Salt or pathogen stress induced *Atbgal1* expression in Arabidopsis[18], but *BGAL* transcription levels in cowpea were decreased under salt treatment[19]. The transcription level of *BGAL* in peaches was also inhibited when subjected to water stress[20].

Longan (*Dimocarpus longan* Lour.) is a tropical/subtropical evergreen fruit tree belonging to the Sapindaceae *Dimocarpus*. Longan is an important economic crop, and its yield and fruit quality were closely related to the development of longan embryos[21]. The difficulty of sampling the early longan zygote embryo greatly limits the application of longan embryo in genetic breeding. The longan somatic embryogenesis (SE) system has the characteristics of genetic stability and high regeneration frequency, which is an ideal material for studying the cell

biology and regulation mechanism of embryogenesis[22]. Chromatin accessibility reflects the contact degree of chromatin DNA with *cis*-acting elements and *trans*-acting factors, while assays for transposase-accessible chromatin sequencing (ATAC-seq) is a sequencing method to capture chromatin accessibility[23]. The study of chromatin accessibility is important for exploring the regulatory network of transcription factors (TFs) and the role of gene expression in plant growth, development and stress resistance[24,25]. Chromatin modification affects chromatin accessibility, which determines the functional state of cells[26]. The monomethylation of histone H3K4 site can be divided into three types: H3K4me1, H3K4me2 and H3K4me3, among which H3K4me1 is usually related to the enhancer[27]. H3K4me1 exhibits highly dynamic changes and is closely related to the cell type specific gene expression profile[28]. In a previous study, Chen et al.[29] revealed the gene regulatory network of cell wall thickening during early longan SE through chromatin accessibility, H3K4me1 modification, and transcriptional analysis. Modification of cell wall components has been validated as key to initiation of cellular responses related to cell fate and development. As a dynamic and complex structure, cell wall plays an important role in regulating plant growth and development, intercellular communication and defense, and determining cell shape and fate[30]. Previous studies have reported that some cell wall components may be markers of cell fate transition, including inducing somatic embryogenesis[31] and postembryonic growth[32]. The *BGAL* family specifically acts on the degradation of pectin, xyloglucan, or arabinogalactose proteins in cell walls, and participates in cell wall metabolism by catalyzing galactose metabolism in the large and complex side chain of the cell wall[33]. During plant maturation, *BGALs* play a significant role in cell wall expansion, degradation and signaling molecule conduction[5,6]. Therefore, investigating of the functional significance of *BGAL* associated cell wall modifications in different cell types and processes is necessary.

In this study, we identified 20 *DlBGAL* genes and analyzed their phylogenetic relationships, conserved motif composition, gene structure and *cis*-acting elements. To determine the role of *DlBGAL* genes in the response to stresses, we evaluated their response to different temperature treatments. *DlBGAL9* was screened by multi-omics analysis and its transcription factors (TFs) regulatory network was predicted. Using luciferase assays and transient expression of *DlAGL61/80* in longan, we investigated the regulatory effect of *DlAGL61/80* on DlBGAL9. The regulation of cell wall thickening by *DlAGL80* and *DlBGAL9* was investigated using longan hairy root system. The results are expected to expand our understanding of the *BGAL* family and further reveal the mechanism of TF-mediated *DlBGAL9* gene during early longan SE.

Materials and methods

Plant materials

The simultaneous embryogenic culture of longan 'Honghezi' in early development consisted of embryogenic callus (EC), incomplete compact pro-embryogenic culture (ICpEC), and globular embryo (GE), which were obtained by adding 2,4-D with 1.0, 0.5 and 0.1 mg/L, respectively[22]. For heat stress (35 °C), the longan EC was transferred to Murashige and Skoog (MS) medium and incubated in dark at 25 and 35 °C, respectively.

The materials were collected at 6, 9, and 12 d of treatment, frozen with liquid nitrogen and stored at −80 °C until use.

Identification of the *DlBGAL* gene family

The longan 'Honghezi' genome database was obtained from the National Center for Biotechnology Information (NCBI) database (PRJNA792504). We conducted systematic BLASTP analysis of longan whole-genome sequences using Arabidopsis BGAL protein sequences (www.arabidopsis.org) in BioEdit software, and confirmed whether the candidate DlBGAL family members had a complete GH35 (PF01301) domain using HMMER[34] (www.ebi.ac.uk/Tools/hmmer/). A total of 20 candidate longan *BGAL* family members were screened. Blast comparison was performed on the NCBI online website (https://blast.ncbi.nlm.nih.gov/Blast.cgi), and members of the DlBGAL family were named with reference to *Citrus*. When multiple DlBGALs matched to the same *Citrus* member, the name was marked -1/2/3/4, according to their physical location (from top to bottom) on chromosomes. The Expasy Protparam (https://web.expasy.org/protparam/) was used to analyze the basic physicochemical properties of the DlBGAL protein.

Phylogenetic, gene structure, and conserved motifs analysis of the *DlBGAL* gene family

Using the BGAL gene protein sequences of longan, Arabidopsis, rice and citrus, a phylogenetic tree was constructed in MEGA 11 (v. 11.0.13) by conducting 1,000 bootstrap replicates with the neighbor-joining (NJ) method[35]. The protein sequences of the Arabidopsis, rice and citrus dates were downloaded from the Ensembl Plants (http://plants.ensembl.org/index.html). The BGAL gene structures were constructed by longan GFF and genome files. Conserved motif analysis of DlBGAL proteins was performed with Multiple Em for Motif Elicitation (MEME) (https://meme-suite.org/meme/tools/meme) using the default parameters. The gene structure and conserved motifs were visualized with TBtools software (Visualize Gene Structure).

Chromosomal localization, synteny and *cis*-acting regulatory elements analysis

The results of chromosome localization information provided by longan GFF file were visualized by Tbtools. MCScanX[36] was used to identify syntenic gene pairs, and BLASTP results and gene location information were used for further input. Tbtools[37] was used to identify proximal, dispersed, tandem, and segmental/whole-genome duplications of *DlBGALs* (Circle gene view). We used PlantCARE (http://bioinformatics.psb.ugent.be/webtools/plantcare/html/) to predict the *cis*-acting elements of *DlBGALs*.

Analysis of the *DlBGAL* gene family by RNA-seq, ATAC-seq, and ChIP-seq

RNA sequencing (RNA-seq), assay for transposase-accessible chromatin sequencing (ATAC-seq), and chromatin immunoprecipitation sequencing (ChIP-seq) assays during early longan SE were available in the NCBI under accession code PRJNA792504. Different temperature treatments were available in the NCBI SRA repository under accession code PRJNA889670.

Dual-luciferase reporter assays in *N. benthamiana* leaves

The *DlBGAL9* promoter (2,000 bp upstream of ATG) was cloned into pGreenII 0800-LUC to produce the reporter construct, while the TFs *DlAGL61_Dlo006037* and *DlAGL80_*

Dlo004817 were cloned into the CaMV35S vector (CaMV35S-DlAGL61/80) as the effector. Primers are listed in Supplemental Table S1. The effector and reporter constructs were mediated into Agrobacterium into *Nicotiana benthamiana* (*N. benthamiana*) by agroinfiltration.

After two days of cultivation, the LUC fluorescence signal was detected using a chemiluminescence imaging system (Gelview 6000Pro II, BLT, China), and the transcriptional activity of the TFs DlAGL61/80 was determined with a Dual-Luciferase Reporter Gene Assay Kit (Yeasen, Shanghai, China) and a Multiskan Spectrum microplate spectrophotometer (BioTek, CA, USA). At least three biological replicates were performed.

Determination of *β*-galactosidase activity, pectin content and ROS accumulation

β-galactosidase activity was determined with the *β*-galactosidase kit (Comin Biotechnology, Suzhou, China). Briefly, 100 mg sample was ground with 1 mL extract for ice bath homogenization. After 4 °C centrifugation (15,000 rcf·min⁻¹ for 10 min), measurement and control were set respectively. Measurement: 10 μL sample mixed 25 μL reagent I and 35 μL reagent II. Control: 10 μL sample mixed 25 μL ddH$_2$O and reagent II. The prepared solution allowed to stand for 30 min at 37 °C before 130 μL Reagent III was added, and the absorbance at 400 nm was determined.

Pectin content was determined with the total pectin content kit (Comin Biotechnology, Suzhou, China). 0.05 g of sample was ground and 1 ml of extract solution I added. The mixed sample was placed at 90 °C for 30 min, and centrifuged at 5,000 g and 25 °C for 10 min after cooling. The supernatant was removed and 1 mL of extract solution I was added to the precipitation, repeating the operation once. After removing the supernatant, 1 mL of extract solution II was added and hydrolyzed at 90 °C for 1 h. After cooling, the sample was centrifuged at 8,000 g and 25 °C for 15 min, and the supernatant was taken for testing. A 30 μl sample was taken and 180 μl concentrated sulfuric acid was added at 90 °C for 10 min, removed and cooled. Thirty μl of reagent III was taken and left to stand at 25 °C for 30 min, then added 60 μl of distilled water. The absorbance at 530 nm was determined.

Reactive oxygen species (ROS) accumulation was determined with the ROS test kit (Comin Biotechnology, Suzhou, China). Briefly, 0.1 g sample was ground with 1 mL reagent I and 10 μL reagent III for ice bath homogenization. After 4 °C centrifugation (600 rcf·min⁻¹ for 5 min), the supernatant was extracted. After 4 °C centrifugation (11,000 rcf·min⁻¹ for 10 min), the supernatant was removed and mixed with reagent II. Measurement and control were set respectively. Measurement: 20 μL sample mixed with 50 μL reagent IV, 50 μL reagent V, 50 μL reagent VI and 30 μL reagent VII. Control: 20 μL reagent II mixed 50 μL reagent IV, 50 μL reagent V, 50 μL reagent VI and 30 μL reagent VII. The mixture was placed in darkness at 37 °C for 30 min, and the absorbance values were measured at the excitation wavelength of 499 nm and the emission wavelength of 521 nm within 10 min.

Transformation of the longan embryogenic callus and hairy root

The genetic transformation of longan EC was mainly through freeze-thaw transformation of recombinant plasmid into Agrobacterium receptor state (GV3101), and transferred of transformed Agrobacterium into LB liquid medium containing antibiotics 100 mg·L⁻¹ Kan and 25 mg·L⁻¹ Rif. The culture was incubated for 18 h at a speed of 200 rcf·min⁻¹ under constant temperature and darkness at 28 °C. Centrifuge at 6,000 rpm for 10 min before removing the supernatant. Added MS liquid medium (including 50 μmol·L⁻¹ AS and 10 μmol·L⁻¹ MgCl$_2$) to resuspend the remaining bacterial solution, and adjusted the bacterial solution OD600 to 0.6–0.8. The cultured longan EC was transferred for about 15 d into the resuspension, incubated for 30 min, and transferred the filtered longan EC to MS solid medium.

According to the method of Meng et al.[38], the longan seedlings were infected with Agrobacterium rhiza. The lateral roots of longan seedlings were removed, and the culture temperature was 26 °C. The seedlings were cultured alternately under light (16 h) and darkness (8 h) for 25 d. A single gene set 100 replicates.

Histological analysis

The hairy roots of longan were cut into small segments and then fixed with FAA [10% formalin, 5% acetic acid, 50% ethanol (v/v)] at ordinary temperature for 48 h. According to the methods of Yang et al.[39], the specimens were dehydrated and infiltrated in the ethanol and paraffin series. After being embedded in paraffin, the samples were cut into semi-thin (1 μm) sections using a microtome (Leica RM2125 RTS, Germany) and stained with 0.1% toluidine blue. Finally, the sections were observed under a microscope (Leica DM2500, Germany).

RNA extraction and qRT-PCR

Total RNA was extracted from longan SE and hairy root using TransZol Up reagent (TransGen, China) and RNAprep Pure Plant Kit (TIANGEN, China), respectively. The cDNA synthesis was performed using the SMART™ RACEcDNA Amplification Kit TransScript RNA First-Strand cDNA Synthesis SuperMix (YEASEN, China). QRT-PCR detection was performed on the Roche Light Cycler 96 instrument, using 10x diluted cDNA as the amplification template. Beta-actin (ACTB) and *ELF-4α* as internal reference genes for transgenic longan EC and hairy root, respectively. The relative expression was calculated by the $2^{-\Delta\Delta Ct}$ method[40], and significant differences were assessed by Duncan test (Student's t-test, *$p < 0.05$, **$p < 0.01$). The data were imported into GraphPad Prism 9 software to generate graphs. Primers are listed in Supplemental Table S1.

Results

Identification and phylogenetic analysis of the longan *BGAL* gene family

To identify the *BGAL* genes in longan, we scanned the *D. longan* genome database using the known BGAL members in Arabidopsis by BLASTP and TBLASTN. After the removal of incomplete and redundant sequences, a total of 20 putative *BGAL* genes were identified in the *D. longan* genome. For the annotation of 20 *DlBGAL* genes, the *Citrus* nomenclature system was pursued with numbers representing the highest sequence similarity with the corresponding CsBGAL orthologous (Table 1). The lengths of amino acids (aa) of 20 DlBGALs range from 444 aa (BGAL13-1) to 889 aa (BGAL9). The MW of DlBGALs varies from 50.15 kDa (BGAL13-1) to 99.79 kDa (BGAL9) with an average of 86.85 kDa. The pI ranged from 5.4 (BGAL8-1) to 9.4 (BGAL13-1). Except for BGAL16-1, the remaining DlBGALs were classified as stable proteins because their instability index was less than 40 (Table 1). The predicted aliphatic index ranged

Table 1. Basic parameter analysis of DlBGAL family.

Gene ID	Gene name	Size (aa)	Molecular weight/kD	PI	Instability coefficient	Hydrophilicity
Dlo000174	BGAL1-1	844	93,311.98	8.25	37.76	−0.287
Dlo000176	BGAL1-2	839	92,852.64	7.96	39.56	−0.267
Dlo000290	BGAL15-1	825	92,233.81	5.56	35.42	−0.444
Dlo002805	BGAL9	889	99,793.27	6.35	35.27	−0.271
Dlo006281	BGAL17	710	79,011.06	6.25	35.45	−0.211
Dlo006300	BGAL1-3	844	93,575.84	8.4	38.83	−0.196
Dlo013472	BGAL5	734	82,104.46	8.8	36.87	−0.276
Dlo014416	BGAL16-1	716	80,274.25	9.34	41.46	−0.262
Dlo014417	BGAL16-2	832	93,191.23	8.62	36.02	−0.416
Dlo015024	BGAL16-3	838	93,942.65	6.32	39.86	−0.208
Dlo015487	BGAL13-1	444	50,149.01	9.4	38.7	−0.233
Dlo015584	BGAL3-1	843	93,502.26	7.25	38.92	−0.221
Dlo016393	BGAL6	718	81,101.64	5.46	36.14	−0.226
Dlo016396	BGAL16-4	846	94,734.74	6.92	40.98	−0.33
Dlo021540	BGAL8-1	842	93,433.6	5.4	39.83	−0.16
Dlo023146	BGAL13-2	864	96,671.78	8.37	36.43	−0.214
Dlo023292	BGAL3-2	660	73,921.74	7.3	34.86	−0.29
Dlo026229	BGAL8-2	853	92,871.32	8.07	39.94	−0.192
Dlo026230	BGAL8-3	612	67,240.37	7.56	36.87	−0.325
Dlo029560	BGAL15-2	828	93,079.31	6.56	34.06	−0.305

from 68.75 to 85.3 in DlBGAL proteins. Due to the GRAVY value (< 0), all DlBGAL proteins were predicted to be hydrophilic.

The phylogenetic tree of the BGAL family contains BGAL gene members from four species: *D. longan*, *O. sativa*, *C. clementina* and *A. thaliana*. To determine their evolutionary relationship, a phylogenetic tree was constructed using the neighbour-joining (NJ) method and tested by 1,000 bootstrap replicates (Fig. 1). According to phylogenetic relationships, the BGALs were clustered into seven groups (Groups I–VII), each containing 4, 2, 6, 1, 3, 3 and 1 DlBGALs, respectively. In *O. sativa*, *A. thaliana* and *C. clementina*, BGAL genes had been identified in cluster forms. Thus, BGAL members may be evolutionarily close in their respective species. Interestingly, BGAL proteins of *O. sativa* and *A. thaliana* and *C. clementina* were clustered into distinct clades (Fig. 1), suggesting that BGAL proteins were evolved after monocots and dicots divergence. Among them, most of the BGAL genes in *D. longan* were closely clustered with *C. clementina* in the groups of the phylogenetic tree, supporting the hypothesis that *D. longan* and *C. clementina* shared close and similar ancestors[41].

Gene structure and motif composition of longan BGAL genes

To further understand the evolutionary relationship of the 20 *DlBGAL* genes, we identified their structural characteristics and motifs (Supplemental Fig. S1). All *DlBGAL* genes had at least 12 exons, with 13 of the 20 genes having more than 18 exons (Supplemental Fig. S1b). The numbers of introns and exons in the genomic sequences were relatively similar in each group. In addition, ten conserved motifs of DlBGAL proteins were identified through MEME analysis (Supplemental Fig. S1c). Motifs 2 and 4, which were components of the DlBGAL domain, were found in all DlBGAL proteins. Motifs 6, 7 and 10 were detected in all DlBGAL proteins except DlBGAL13-1. For group III, IV and VI, all of the DlBGALs possessed 10 motifs (Supplemental Fig. S1c).

Chromosomal location and gene duplication events of *DlBGAL* genes

The chromosome information of *DlBGAL* genes was extracted and the chromosomal positions indicated that *DlBGAL* genes

were distributed on eight of the 15 chromosomes of longan (Fig. 2a). Among them, Chr1, 6 and 7 had four *DlBGAL* genes. Chr3, 11 and 12 had two *DlBGAL* genes, while the Chr10 and 14 had the smallest numbers of *DlBGAL* genes (one gene each). The distribution of *DlBGAL* genes was uneven.

The results of collinearity analysis showed that there were six pairs of segmental duplication events in *DlBGALs*, corresponding to *DlBGAL1-1/1-3*, *DlBGAL5/3-1*, *DlBGAL5/3-2*, *DlBGAL16-1/6*, *DlBGAL13-1/13-2* and *DlBGAL3-1/3-2* (Fig. 2a). The paralogous gene pairs were distributed on different chromosomes, which may be beneficial for the evolution and expansion of the *DlBGAL* gene family. The expansion of the *DlBGAL* gene family was mainly due to segmental duplication, rather than tandem duplication. To verification the evolutionary rates and selective pressures between the *DlBGAL* genes and their duplicated genes, we used Ka (nonsynonymous), Ks (synonymous), and the Ka/Ks ratio for estimations. As shown in Supplemental Table S2, the Ka/Ks values of all the *DlBGAL* gene pairs were less than 1, indicating that the *DlBGAL* gene family underwent strong purifying selection. These results indicated that *DlBGAL* family was conservative during the domestication process of longan.

The collinearity analysis between longan and *Arabidopsis thaliana* or *Oryza sativa* showed that three *DlBGAL* homologue genes appeared in the three chromosomes of *Oryza sativa*, but 16 *DlBGALs* had corresponding paralogous genes on five chromosomes in *Arabidopsis thaliana* (Fig. 2b). The relationship between longan and *Arabidopsis thaliana* was closer than that between longan and *Oryza sativa*.

Analysis of *cis*-elements in the promoter region of *DlBGAL* genes

The *cis*-elements are involved in the regulation of gene expression, which are an important part of the response regulation network for plant growth and development, hormone response and stress response[42,43]. We isolated the 2-kb upstream promoter region of the *DlBGAL* genes to identify the potential *cis*-elements. Among them, many *DlBGAL* genes exhibit elements specifically related to light signaling, hormone, stress and development.
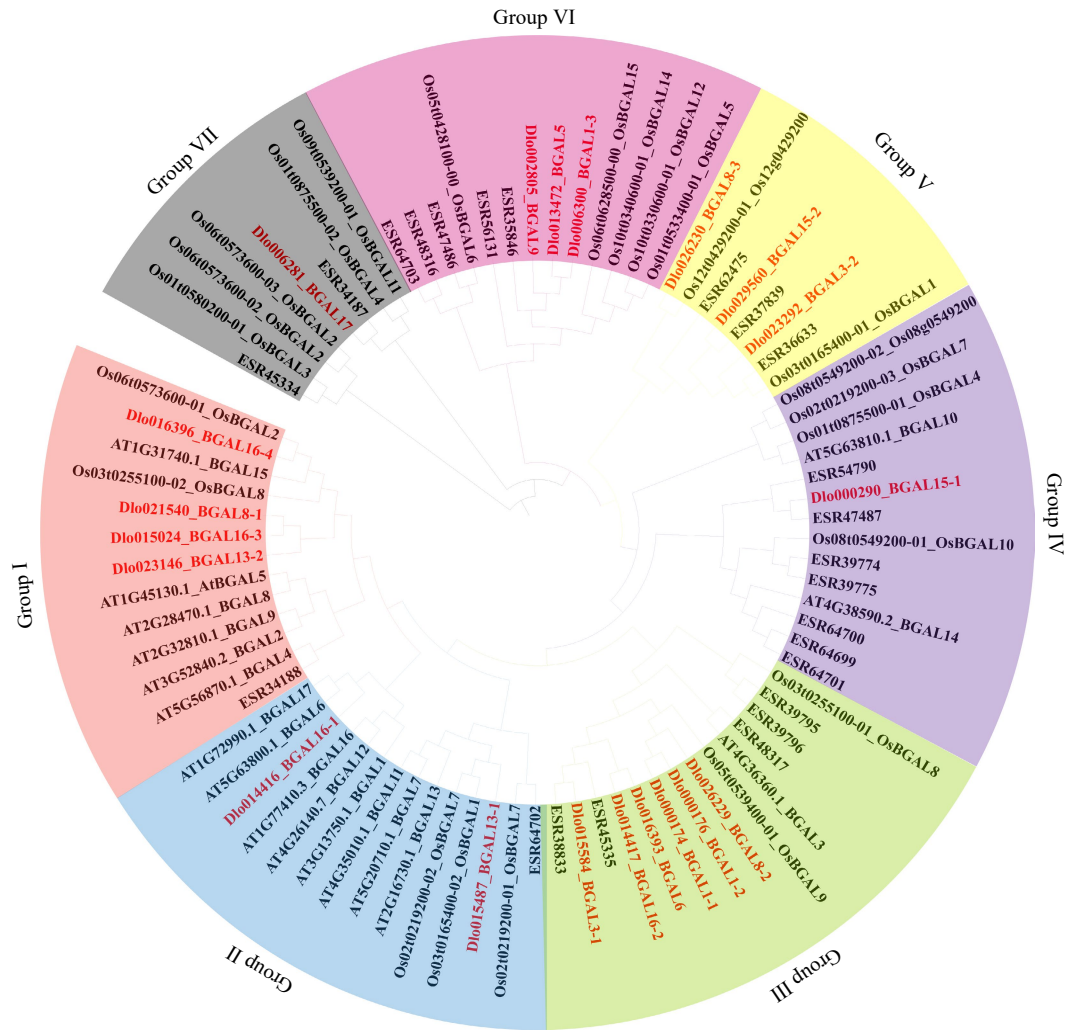
Fig. 1 Phylogenetic tree analysis of *β*-galactosidase (BGAL) proteins from longan, *Citrus*, *Arabidopsis*, and *Oryza*.

For *DlBGAL* genes, 34 main types of *cis*-elements were identified in their promoter sequences, which included 11 light responsive, 10 hormone responsive, seven stress responsive, and six development elements (Fig. 2c). The major light responsive elements were Box4 and G-box and the most common motifs were the JA-responsive elements (MYC), abscisic acid (ABA)-responsive element (ABRE), and ethylene-responsive element (ERE) of the scanned hormone responsive motifs. MYB and ARE were the most *cis*-elements of the stress responsive. These results suggested that *DlBGAL* genes were participated in complex light, hormone regulation and stress responsive networks that may involve multiple regulatory modalities.

Expression analysis of *DlBGAL* genes during early SE and under different temperature stress conditions

The expression profiles of *DlBGAL* genes during early SE and under temperature treatments were illustrated using our previous RNA-seq dataset. Results showed that nine *DlBGALs* (*DlBGAL8-3/15-1/13-2/16-2/15-2/13-1/8-1/6/3-2*) were almost not expressed (FPKM < 1) in the early SE RNA-seq dataset (Fig. 3a). About the remaining 11 genes, there were four genes (*DlBGAL17/16-3/1-2/16-1*) that showed high expression levels at EC stage and six genes (*DlBGAL1-1/16-4/9/8-2/1-3/3-1*) had high

expression levels at GE stage. Furthermore, only *DlBGAL5* was presented high expression at ICpEC stage. These results suggested that the *DlBGAL* genes may be involved in promoting early SE. The differentially expressed date of *DlBGAL* genes under different temperature conditions were derived from the RNA-seq (Fig. 3b). From the results, the expression levels of some *DlBGAL* genes varied obviously under high-temperature and low-temperature treatments. Compared to normal culture temperature (25 °C), seven *DlBGAL* genes (*DlBGAL3-2/1-2/16-2/17/5/1-1/16-3*) were upregulated under the high-temperature and two *DlBGAL* genes (*DlBGAL5/1-1*) were upregulated at low-temperatures.

The change of chromatin accessibility affects the binding of transcription factors and other protein molecules to chromatin, thereby regulating gene transcription[44]. ATAC-seq analysis revealed that chromatin accessibility of other *DlBGAL* genes, except *DlBGAL17* and *DlBGAL8-3*, was open during the early SE (Fig. 3c). Histone methylation modification can activate or inhibit gene transcription by the state of methylation, in which H3K4me1 is a marker associated with enhancers[45]. Except for *DlBGAL6*, H3K4me1 binding peaks were detected in other *DlBGAL* genes during early SE, and most of them had binding peaks at three stages. Combined with transcription, chromatin accessibility, and H3K4me1 modification results, most *DlBGAL*
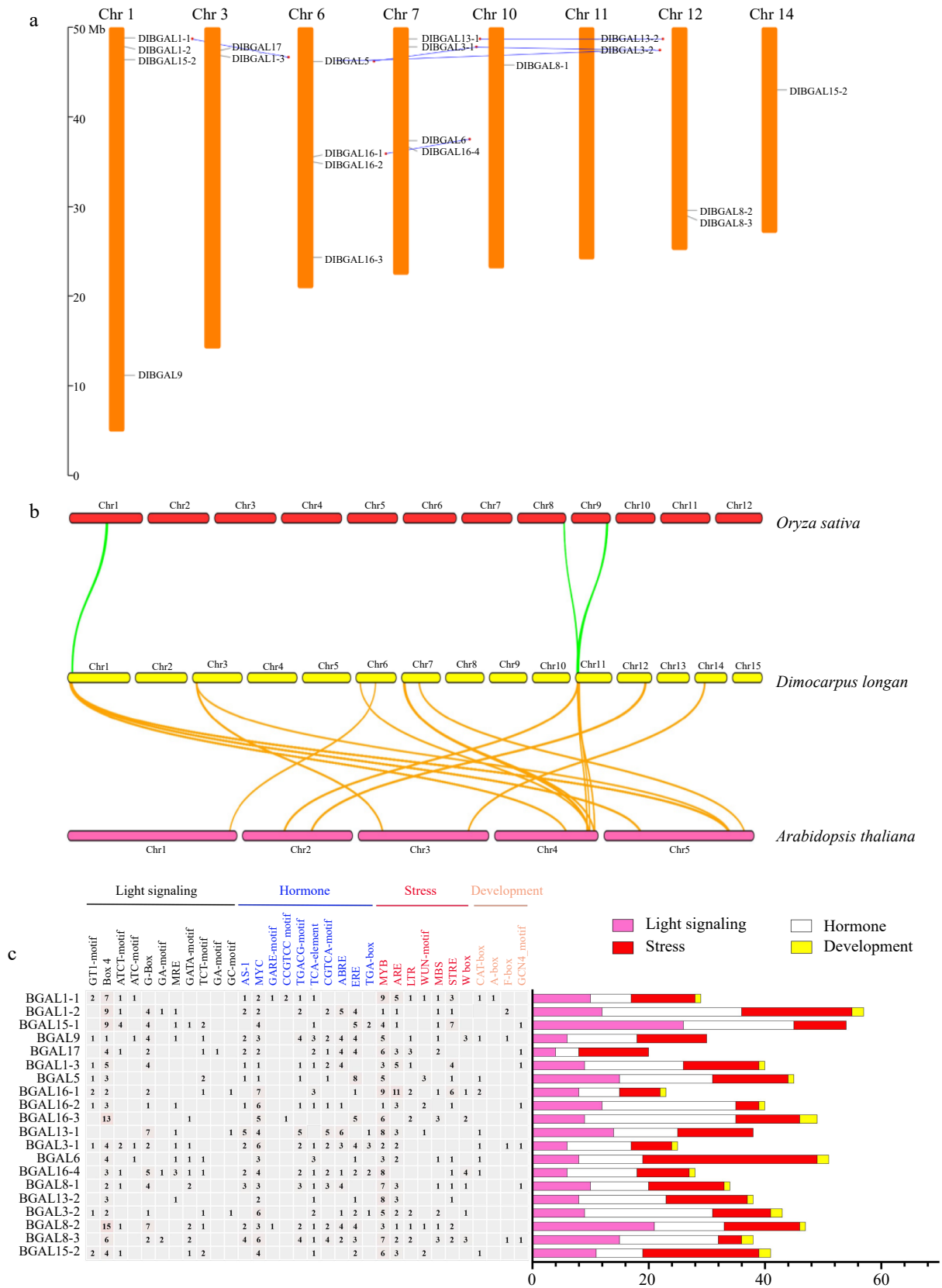
Fig. 2 Chromosomal distribution, synteny and *cis*-elements analysis of *DlBGAL* genes. (a) Distributions and duplications of DlBGAL genes along longan chromosomes. The gray and blue lines indicate chromosome locations of *DlBGALs* and segmentally duplicated genes, respectively. (b) The homologous relationships of *BGAL* genes in longan, *Oryza* and *Arabidopsis*. The green and orange lines indicate the homologous relationships of *BGAL* genes with *Oryza* and *Arabidopsis*, respectively. (c) Analysis of *cis*-elements in the promoter of *DlBGAL* genes. Heatmap of the numbers of *cis*-elements in the promoters of *DlBGAL* genes.
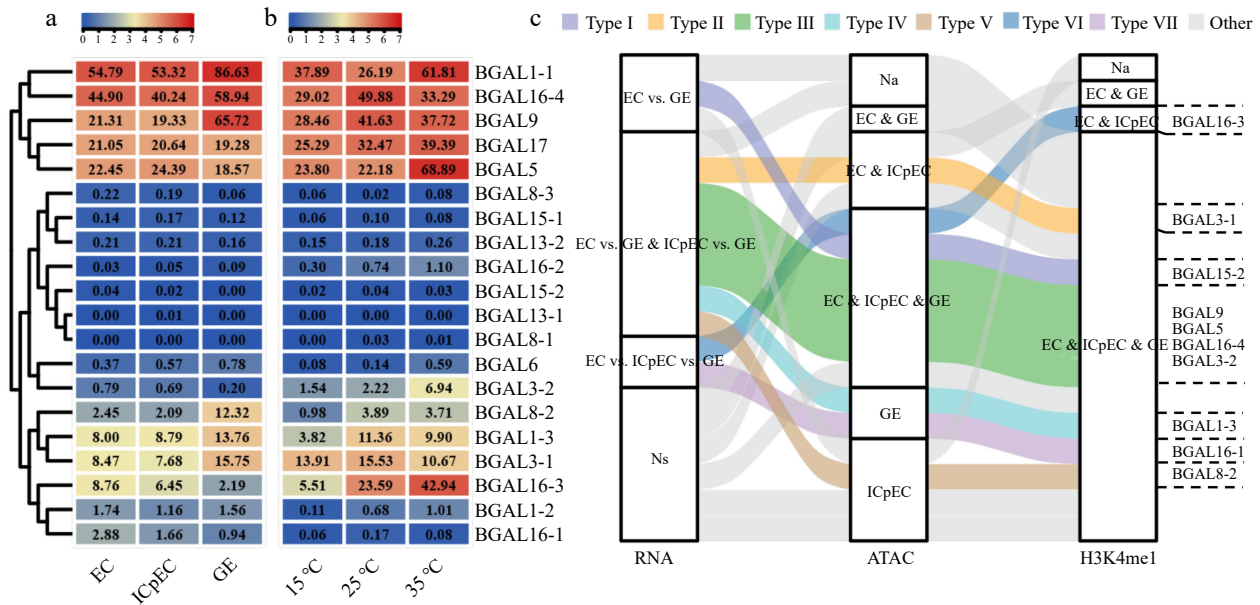
Fig. 3 Expression profile and multi-omics analysis of *DlBGAL* genes. (a), (b) Expression analyses of *DlBGAL* genes during early longan SE and different temperature treatments. (c) Alluvial diagram of *DlBGAL* genes was divided into eight types (types I–VII and other) based on ATAC-seq, ChIP-seq, and RNA-seq data. The width of different colored bars represents the number of genes, and the genes included in each type were listed in the right panel. EC vs GE, the differential expression of EC vs GE; EC vs GE & ICpEC vs GE, the differential expression of EC vs GE and ICpEC vs GE; EC vs ICpEC vs GE, the differential expression of EC vs ICpEC, ICpEC vs GE and EC vs GE; ICpEC/GE, ATAC-seq or ChIP-seq (H3K4me1) peaks were detected in ICpEC/GE; EC & ICpEC, ATAC-seq or ChIP-seq (H3K4me1) peaks were detected in EC and ICpEC; EC & ICpEC & GE, ATAC-seq or ChIP-seq (H3K4me1) peaks were detected in EC, ICpEC and GE; Na, undetectable peak of ATAC-seq or ChIP-seq (H3K4me1); Ns, no difference in transcripts among the samples.

genes differentially expressed during early SE could be detected in the ATAC-seq and ChIP-seq data. In summary, multi-omics analysis has implications for the potential mechanism of *BGAL* family involvement in early SE.

Transcription factors target the *DlBGAL9* promoters and activate its transcription

Transcription factors (TFs) can inhibit or enhance gene expression, and promote SE formation by directly activating early embryonic model genes[24]. To understand the regulatory network of transcription factors on *DlBGAL* genes, the upstream 2-kb sequences of *DlBGAL* genes were used as TF binding regions. In total, 11 *DlBGALs* were predicted as targets for 10 TFs (Fig. 4a). Based on multi-omics analysis, the functional role of *DlBGAL9* in early longan SE attracted further interest. Previous studies have identified an important somatic embryo marker gene, *Dlo004817_AGL80*, which was involved the regulatory network associated with the cell wall of longan[29]. Based on TFs and DlBGALs regulatory network, Dlo006037_DlAGL61 and Dlo004817_DlAGL80 were selected as candidate TFs for regulating *DlBGAL9* (Fig. 4a).

To investigate the regulatory effect of DlAGL61/80 on *DlBGAL9* transcription, we verified the expression of *DlBGAL9* in longan EC that overexpressed TFs *DlAGL61/80*. QRT-PCR results showed that *DlBGAL9* expression was significantly increased in longan EC with overexpressing of *DlAGL61* (3.19-fold) and *DlAGL80* (8.87-fold) (Fig. 4b). Thus, TFs *DlAGL61/80* may enhance DlBGAL9 transcription by targeting its promoters. To further verify whether TFs *DlAGL61/80* can activate the expression of *DlBGAL9*, a luciferase (LUC) reporter assay was performed in *Nicotiana benthamiana* leaves. Two constructs, *35S::DlAGL61* and *35S::DlAGL80* were used as effector, and

DlBGAL9pro:LUC was used as reporter (Fig. 4c). Compared with control check (CK), the relative *DlAGL61/80*-induced firefly LUC/Renilla luciferase (REN) activity driven by the promoters of DlBGAL9 increased 1.41-fold and 1.86-fold, respectively (Fig. 4d, e). These results indicated that TFs DlAGL61/80 may target the *DlBGAL9* promoters and activate their transcription.

Transcription factors and *DlBGAL9* responses to heat stress and changes of β-galactosidase activity and pectin content during early longan somatic embryogenesis

Based on the RNA-seq data of longan EC under temperature treatments, *DlBGAL* genes expression detected in early longan SE responded to heat stress (Fig. 3b). Previous studies have found that heat stress affects the process of early longan SE, and EC cannot develop to GE under 35 °C treatment (heat stress). To further investigate the response of *DlBGAL9* and TFs *DlAGL61/80* to heat stress, we detected their expression of longan EC treated at 35 °C. The results showed that *DlBGAL9* was significantly upregulated under heat stress at 6 d, and the TF *DlAGL61* showed a significant downregulation trend under heat stress at 9 d (Fig. 5a). Notably, *DlBGAL9* and TFs *DlAGL61/80* have the highest level under heat stress at 12 d (Fig. 5a). The *DlBGAL9* and TFs *DlAGL61/80* showed a similar trend under heat stress, indicating that the DlAGL61/80-DlBGAL9 regulatory network may be involved in longan's response to heat stress.

To further analyze the role of β-GAL and pectin during early longan SE, the changes in β-GAL activity and pectin content were measured (Fig. 5b, c). The β-GAL activity was significantly upregulated during early longan SE (Fig. 5b). Pectin content was opposite to β-GAL activity, and the highest pectin content
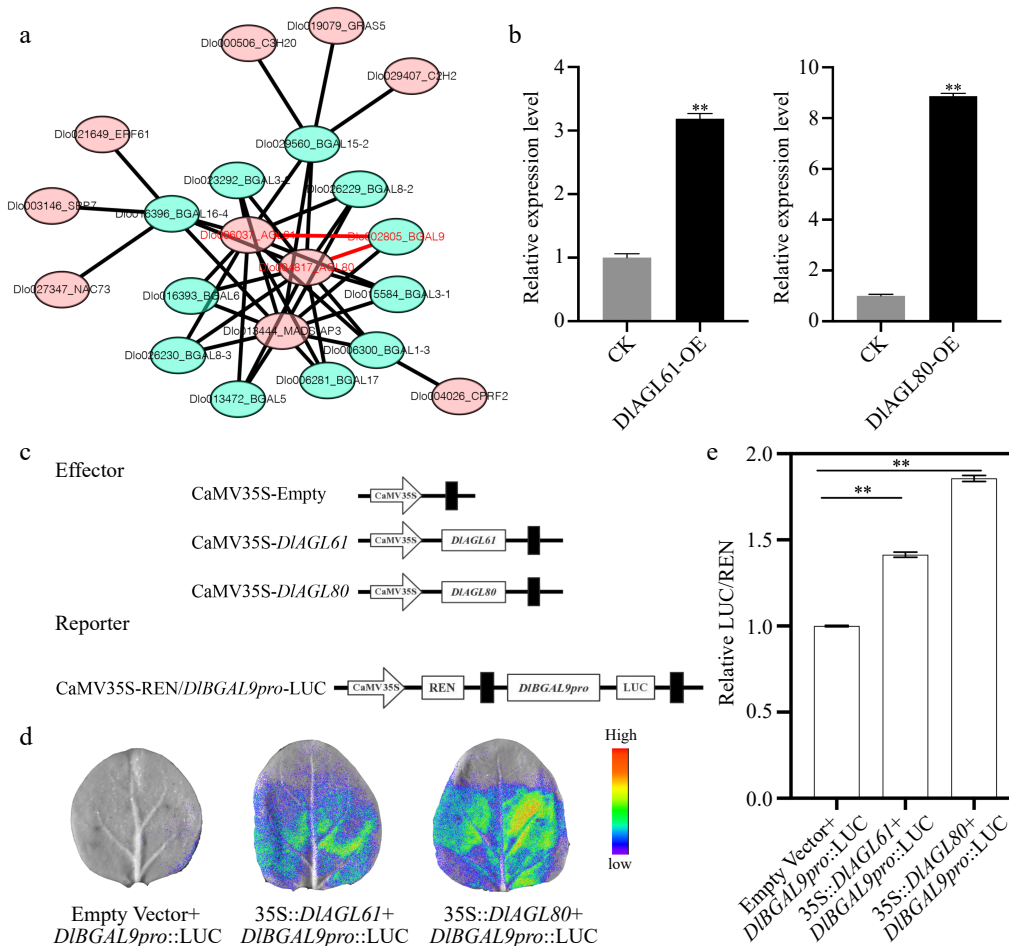
Fig. 4 Transcription factors (TFs) regulate the expression of *DlBGAL9*. (a) Network prediction of *DlBGAL* gene regulated by TFs. The red font represents the key genes. (b) The relative expression of *DlBGAL9* in the TFs *DlAGL61/80* transiently transformed. Beta-actin (ACTB) was used as a reference gene to normalize gene expression data. Each treatment was conducted in triplicate with three technical repeats. (c) Schematic diagrams of the effector vectors and reporter vectors in luciferase assays. (d) The interactions of DlAGL61 or DlAGL80 with the *DlBGAL9* promoter that were detected in leaves of *N. benthamiana* through a dual luciferase reporter system. (e) Determination of the luciferase enzyme activity in *N. benthamiana*. Values were mean ± SD. **indicates a statistically significant difference, **$p < 0.01$.

was found in the EC stage (Fig. 5c). After that, the β-GAL activity of longan ECs treated at heat stress for different durations was determined. Compared with the normal temperature (25 °C), the β-GAL activity was significantly downregulated at 6 and 12 d of heat stress (35 °C) and significantly increased at 9 d (Fig. 5d). It was suggested that β-GAL can not only participate in somatic embryonic process by negatively regulating pectin content, but also can respond to heat stress.

Overexpression of *DlBGAL9/DlAGL80* thickens the root cell wall by affecting β-GAL activity

As the embryonic callus is composed of parenchyma cells, it poses certain obstacles to the study of cell walls. Hairy roots have the characteristics of rapid growth and hereditary stability, providing a good material for studying the impact of genes on cell walls. In this study, the constructed p1302: DlBGAL9: GFP was introduced into the Agrobacterium rhizogenes strains and transferred into longan seedlings. The GFP-signals and PCR results both confirmed that *DlBGAL9* had been transferred into longan seedlings and successfully induced the hairy roots (Fig. 6a). Compared with the wild-type (WT), transgenic roots overexpressing *DlBGAL9* (*DlBGAL9*-OE) showed a 24.20-fold increase in *DlBGAL9* expression (Fig. 6a). We examined the β-GAL

activity and pectin content in the transgenic hairy roots (Fig. 6b, c). The β-GAL activity of *DlBGAL9*-OE root was higher, while the pectin content was lower. These results suggested that *DlBGAL9* influences pectin content by regulating β-GAL activity in transgenic hairy roots.

As DlAGL80 target the *DlBGAL9* promoters and activate its transcription, we tested whether the expression of *DlBGAL9* was affected by *DlAGL80* transgenic roots. The overexpressing *DlAGL80* (*DLAGL80*-OE) transgenic hairy roots was confirmed by GFP-signals and PCR results, and the expression of *DlAGL80* increased by 9.61-fold (Fig. 6d). In *DlAGL80*-OE roots, *DlBGAL9* expression was dramatically increased, while β-GAL activity was increased (Fig. 6e, f). Transverse sections of *DlBGAL9* and *DlAGL80* transgenic hairy roots showed thickening of cell walls in both genotypes compared to WT (Fig. 6g). In summary, *DlAGL80* may regulate the expression of *DlBGAL9* by regulating β-GAL activity and participate in the cell wall modification processes.

DlBGAL9 and TF *DlAGL80* overexpression enhances the resistance to heat stress

The expression of *DlBGAL9* and TF *DlAGL80* in roots under heat stress were assessed to investigate whether *DlBGAL9* and
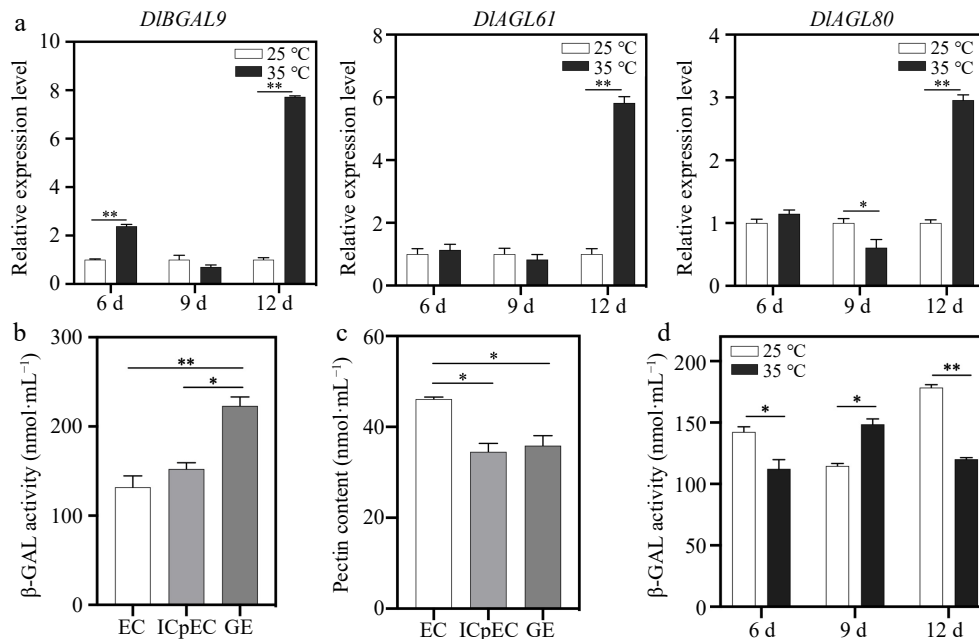
Fig. 5 Expression pattern analysis of *DlBGAL9* and TFs *DlAGL61/80* in longan EC under heat stress. (a) Expression of *DlBGAL9* and TFs *DlAGL61/80* in longan EC under different days of heat stress. Beta-actin (ACTB) was used as a reference gene to normalize gene expression data. (b) The *β*-GAL activity during early longan somatic embryogenesis (EC, ICpEC, and GE). (c) The pectin content during early longan somatic embryogenesis (EC, ICpEC, and GE). (d) The *β*-GAL activity in longan EC under different days of heat stress. Somatic embryos were cultured on MS medium and treated at 25 °C (normal) and 35 °C (heat stress). Samples were harvested after 6, 9, and 12 d to detect the gene expression patterns and *β*-GAL activity. MS, Murashige and Skoog medium. EC, embryogenic callus; ICpEC, incomplete compact pro-embryogenic culture; GE, globular embryo. Each treatment was conducted in triplicate with three technical repeats. Values are mean ± SD. * Indicates a statistically significant difference, *$p < 0.05$, **$p < 0.01$.

TF *DlAGL80* were involved in the resistance of longan roots to heat stress. QRT-PCR results showed that heat stress induced *DlBGAL9* and TF *DlAGL80* expression, which reached the peak value at 6 d (Fig. 7b). Further results showed that the hairy root cell wall of longan was thickened under heat stress (Fig. 7a). The above results indicated that *DlBGAL9* and TF *DlAGL80* may participate in the mechanism of longan resistance to heat stress. When plants were subjected to biotic or abiotic stress, the concentration of reactive oxygen species (ROS) in cells increases and the homeostasis of cells was destroyed. The activity of ROS scavengers (SOD, POD and CAT) will increase accordingly to maintain the homeostasis of cells. Fe-SOD (FSD) and Mn-SOD (MSD) belong to the super oxide dimutese (SOD) gene family. The expression of SOD, peroxidase (POD) and catalase (CAT) related genes in *DlBGAL9*-OE/*DlAGL80*-OE roots were significantly upregulated (Fig. 7c). In summary, *DlBGAL9* and TF *DlAGL80* may reduce the damage caused by heat stress to longan hairy roots by regulating the content of SOD, POD and CAT.

Discussion

The *DlBGAL* gene family exhibits evolutionary conservation and functional diversity

Plant *BGAL* family is widely involved in cell wall structure, intercellular protein modification[11,12], and plant growth and development[46,47]. In this study, 20 *BGAL* family members were identified in 'Honghezi' longan, which was similar to the number of *Arabidopsis thaliana* (17 *AtBGALs*)[48], *Solanum lycopersicum* (17 *SlBGALs*)[48], *Prunus persica* (17 *PpBGALs*)[46] and *Oryza sativa* (23 *OsBGALs*)[8], but less than that of *Linum*

usitatissimum (43 *LuBGALs*)[49] and *Brassica juncea* (39 *BjuBGALs*)[50]. The protein sequence of the GH35 active site is the site of *β*-galactosidase specific binding substrate, so the absence and incompleteness of this site may be related to the loss of enzyme activity. Except for *DlBGAL13-1* and *DlBGAL8-3*, all *DlBGAls* possess the typical GH35 active site sequence GGP[LIVM]xQxENE[FY]. In Arabidopsis, *AtBGAL1~AtBGAL6*, *AtBGAL10* and *AtBGAL12* contain GH35 active sites[48]. In sweet-potato, GH35 active sites were detected in all members of except *Ibbgal13*[10]. However, the GH35 active sites of *BGAL* family were missing or incomplete in plants such as *Brassica junce*, Chinese cabbage, flax and cotton. In the longan *BGAL* family, introns were identified to be numerous and dense. Similar to studies in other species, it is speculated that members of the *BGAL* family may be more affected by regulatory elements.

Phylogenetic trees showed that the BGAL proteins of longan and citrus were more closely related. *Cis*-elements are involved in the regulation of gene expression, which is an important component of the response regulatory network for plant growth and development, hormone response, and stress response[42,43]. *Cis*-acting elements of the *DlBGAL* promoter revealed that most of them contain elements related to light signaling, hormones, stress, and development. Studies have found that ethylene can inhibit the transcription of *PaGAL3* and *PaGAL4* in avocado fruits, as well as the relationship between auxin induced plant embryo elongation and *β*-galactosidase activity. In addition, the transcription of *BGAL* is associated with salt stress, drought stress, and pathogen infection. In summary, *BGAL* family members may participate in various regulatory networks such as signal transduction and stress response during the growth and development of longan.
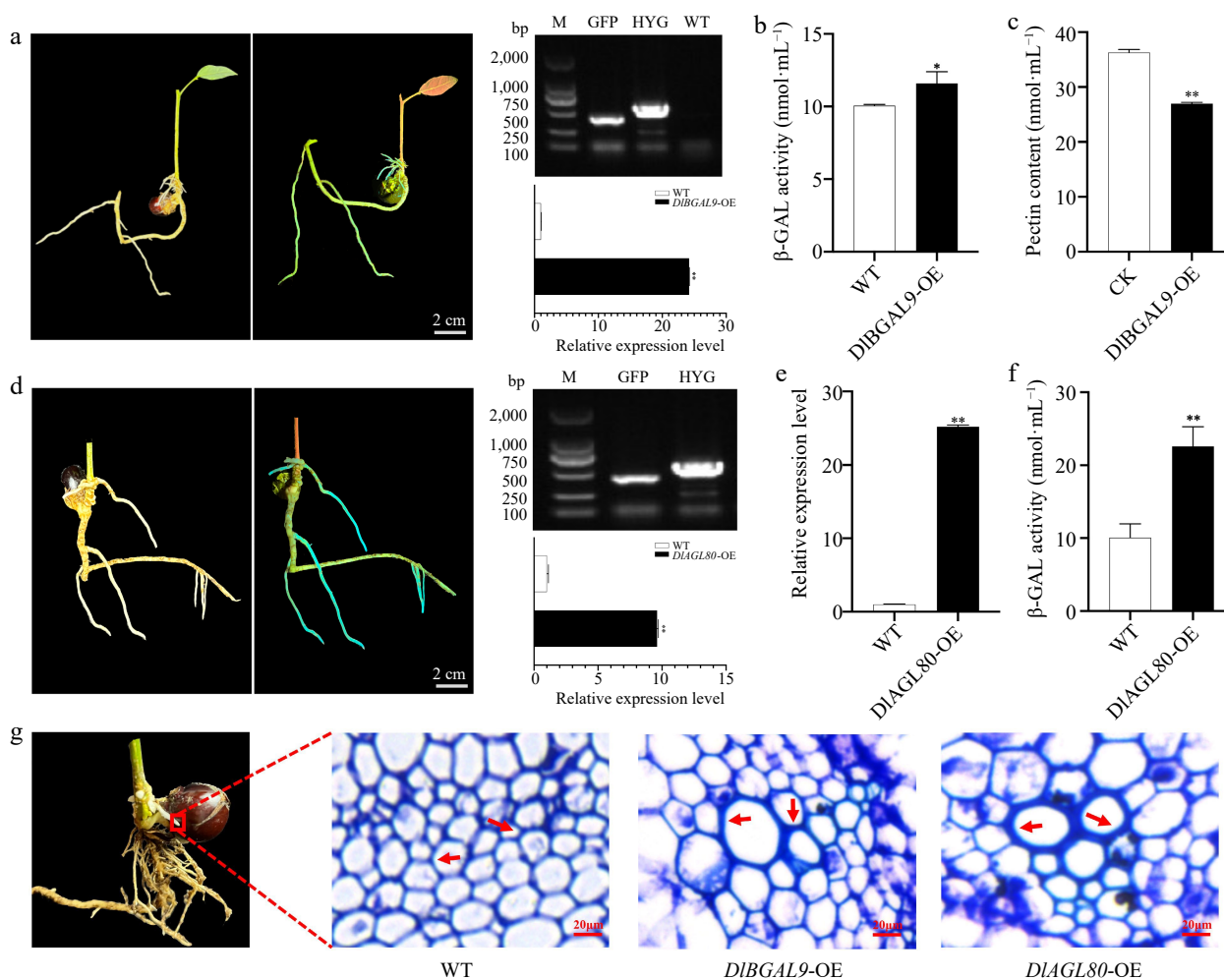
Fig. 6 Functional analysis of *DlBGAL9* and TF *DlAGL80* in longan hairy root. (a) Left: The bright field and GFP-fluorescent *DlBGAL9*-OE transgenic hairy roots. Right: Molecular identification *DlBGAL9*-OE transgenic hairy roots. Scale bar = 2 cm. (b) The β-GAL activity in longan hairy root of *DlBGAL9*-OE transgenic. (c) The pectin content in longan hairy root of *DlBGAL9*-OE transgenic. (d) Left: The bright field and GFP-fluorescent longan hairy root of the *DlAGL80*-OE transgenic. Right: Molecular identification longan hairy root of the *DlAGL80*-OE transgenic. Scale bar = 2 cm. (e) Expression of *DlBGAL9* in longan hairy roots of *DlAGL80*-OE transgenic. (f) The β-GAL activity in longan hairy roots of *DlAGL80*-OE transgenic. (g) Anatomical and morphological observations of WT, *DlBGAL9*-OE and *DlAGL80*-OE longan hairy roots. Arrows indicate the position of cell wall thickening. Scale bar = 20 μm. (*$p < 0.05$, **$p < 0.01$).

DlAGL61/DlAGL80 activate the expression of DlBGAL9 and participated in the regulation of longan somatic embryogenesis

The remodeling of cell wall polysaccharide networks is an important process in plant growth and response to external signals[51]. Pectin is a polysaccharide that helps maintain cell wall porosity and cell adhesion. Pectin has the ability to bind to ions, growth factors and enzymes, and is involved in cell differentiation and elongation[52,53]. More and more evidence suggests that cell wall components like pectin and arabinogalactan-proteins play a crucial role in plant somatic and zygotic embryogenesis[54,55]. *BGALs* belong to the GH35 family and are widely involved in cell wall structure, modification of intercellular connections, and cell wall metabolism. In this study, six of the 11 *DlBGALs* whose expression were highly expressed in GE, and it is speculated that these *DlBGAL* genes may be conducive to promoting early SE. Similarly, transcription of all *BGAL* members in Arabidopsis occurs during early development[14], and *CanBGal-5* in chickpea was associated with high cell division rate growth[16]. Based on the above

results, it was speculated that the *DlBGALs* may participate in the process of SE through cell wall modification.

MADS-box genes encode a large transcription factor family in eukaryotes, widely considered as a regulatory factor involved in reproductive development, floral transformation, and organ identity[56]. We selected *DlBGAL9* and two MADS-box genes (*DlAGL61* and *DlAGL80*) of 10 TFs that based on RNA-seq. To understand the relationship between TFs *DlAGL61/80* and *DlBGAL9*, we transiently transformed *DlAGL61* and *DlAGL80* into longan EC. The results confirmed that TFs *DlAGL61* and *DlAGL80* significantly increased the expression of *DlBGAL9*. We further verified that the TFs *DlAGL61/80* could enhance the expression of DlBGAL9 by a LUC reporter assay performed in *Nicotiana benthamiana* leaves. These results showed that *DlAGL61* and *DlAGL80* enhance the expression of *DlBGAL9* to different extents. *GmAGL15* was preferentially expressed in embryos during soybean development, and overexpression of *GmAGL15* promotes soybean somatic embryo development[57]. In tomato, *DkGAL1* was involved in seed germination and radicle elongation[58]. The above results further confirmed that the TFs
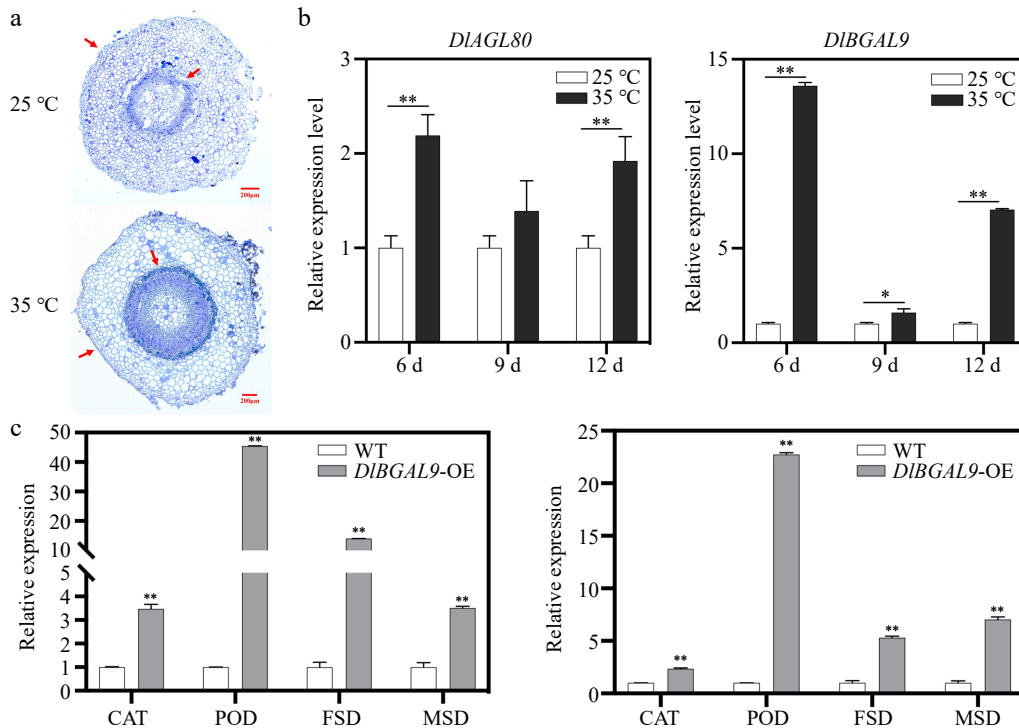
Fig. 7 Expression pattern analysis of *DlBGAL9* and *DlAGL80* under heat stress in longan hairy root. (a) Anatomical and morphological observations of longan hairy root under heat stress. Arrows indicate the position of cell wall discrepancy. (b) Expression pattern analysis of *DlAGL80* and *DlBGAL9* under different days of heat stress in longan hairy root. (c) Expression profiles of ROS pathway related genes in WT, *DlBGAL9*-OE and *DlAGL80*-OE longan hairy roots. (*$p < 0.05$, **$p < 0.01$).

DlAGL61 and *DlAGL80* could enhance the expression of *DlBGAL9* and participate in the regulation of longan SE.

DlAGL80 promote DlBGAL9 expression to thicken the cell wall and respond to heat stress

In plants, *BGAL* regulates cell wall remodeling and occurrence by regulating polysaccharide metabolism of cell wall components[59]. In Arabidopsis, all *BGAL* genes were expressed in the cell wall. Dean et al.[60] observed *BGAL6* localization on the cell wall through subcellular localization. Gantulga et al.[61] detected the localization of BGAL2 and BGAL5 on the cell wall by dotblotting, while Hui et al.[62] detected the localization of BGAL8 on the cell wall by proteomics. Gantulga et al.[63] showed that *BGAL1* and *BGAL12* were present in the xylem thickened cell walls through immunogold labeling followed by transmission electron microscope of root sections. *AGL* regulates the development of eukaryotes by participating in cell proliferation and differentiation. *AGL21* plays a crucial role in the growth process of Arabidopsis lateral roots[64]. The number of lateral roots in mutant *agl21* decreases, while overexpression of *AGL21* can increase the number of Arabidopsis lateral roots[64]. In this study, the longan transgenic hairy roots of *DlBGAL9*-OE and *DlAGL80*-OE promoted the accumulation of *β*-GAL enzyme activity and cell wall thickening. According to the above results, it is speculated that *DlAGL80* regulates the *β*-GAL enzyme activity by regulating the expression of *DlBGAL9*, and then participates in the modification of cell wall. In addition, the pectin content in *DlBGAL9*-OE hairy roots was significantly downregulated. The many roles of pectin in plant development. Genes relevant to pectic homogalacturonan biosynthesis, modification and degradation are expressed with spatiotemporal specificity and respond to intrinsic growth and environmental cues throughout the plant life cycle. They function in many developmental processes by regulating cell wall composition, structure and mechanical properties[65]. Meanwhile, cell wall pectin, cellulose, and cytoskeleton synergistically regulate the molecular mechanisms of cell wall integrity and plant growth and development[66]. Therefore, overexpression of the AGL61/80-BGAL9 module may lead to a more complex regulatory mechanism for cell wall thickening.

Global warming has affected plant growth and development[67]. Previous studies have found that heat stress inhibits the normal somatic embryogenesis of longan[68]. In RNA-seq data of treated at different temperatures, it was found that most of the detected *DlBGAL* genes were upregulated at heat stress. Interestingly, the expression of *DlBGAL9* and TFs *DlAGL61/80* was significantly upregulated at 12 d of heat stress (35 °C) in longan EC, while *β*-GAL activity was significantly downregulated. This may be due to the poor thermal stability of *β*-GAL[69]. Some studies have found that the *BGAL* family is also regulated by biological and abiotic stresses[17], including salt stress[18], water stress[20] and pathogen stress[18]. It was speculated that *DlBGALs* may participate in stress response during SE through cell wall modification. Heat stress may lead to lower ion concentrations in cell fluid and promote the production of ROS and other toxic compounds. Excessive ROS accumulation can seriously affect plant growth and development, reduce plant cell viability, and programmed cell death[70,71]. At the same time, the activity of SOD, CAT, and POD increases to maintain intracellular homeostasis[72]. In this study, qRT-PCR was used to analyze the expression patterns of EC and hairy roots of *DlBGAL9* and *DlAGL80* in longan under heat stress. Under heat stress, the expression levels of *DlBGAL9* and
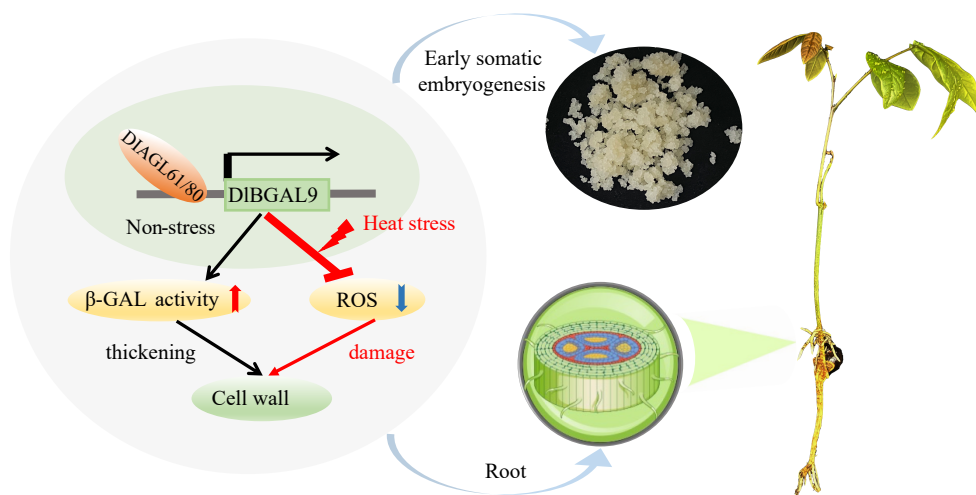
Fig. 8 Proposed model of the underlying mechanism *via* which TFs *DlAGL61/80* and *DlBGAL9* regulate early somatic embryogenesis and responding to heat stress in longan. *DlAGL61/80* activate the expression of *DlBGAL9,* leading to upregulation of β-GAL activity and thickening of cell walls. Reduce the content of ROS and reduce damage under heat stress. Arrow for promotion and blunt ends indicate inhibition, respectively. Red arrow represents upregulation of β-GAL activity and blue arrow represents downregulation of ROS content.

DlAGL80 were upregulated, while the β-GAL activity was decreased. In addition, SOD, CAT and POD related genes were upregulated in overexpressed *DlBGAL9* and *DlAGL80* longan hairy roots. In summary, *DlBGAL9* and *DlAGL80* may respond to the process of heat stress of longan by regulating ROS accumulation.

Conclusions

In this study, 20 *BGAL* genes were identified in the longan genome. The expression patterns of *DlBGAL* genes in early SE and stresses responses were different, which coordinately promoted the process of early SE and resistance to heat stress. We screened *DlBGAL9* at the transcriptional level and verified that TFs *DlAGL61/80* can promote the expression of DlBGAL9. In addition, it was verified that *DlAGL80* promote DlBGAL9 expression to thickens cell wall and respond to heat stress. These findings provide a model in which *DlAGL80* regulation of *DlBGAL9* enhances β-GAL activity to promote cell wall modification during early longan SE and responses to heat stress (Fig. 8).

Author contributions

The authors confirm contribution to the paper as follows: study conception and design: Lin Y, Lai Z; data collection: Xu L, Lai C, Zhang X, Guan Q, Zhang Z, Chen Y; analysis and interpretation of results: Chen Y, Ma X, Ma W; draft manuscript preparation: Chen Y, Ma X. All authors reviewed the results and approved the final version of the manuscript.

Data availability

All data generated or analyzed during this study are included in this published article and its supplementary information files.

Conflict of interest

The authors declare that they have no conflict of interest.

References

1. Smith DL, Gross KC. 2000. A family of at least seven β-galactosidase genes is expressed during tomato fruit development. *Plant Physiology* 123:1173−84

2. Cantarel BL, Coutinho PM, Rancurel C, Bernard T, Lombard V, et al. 2009. The Carbohydrate-active EnZymes database (CAZy): an expert resource for Glycogenomics. *Nucleic Acids Research* 37:D233−D238

3. Dwevedi A, Kayastha AM. 2010. Plant β-galactosidases: physiological significance and recent advances in technological applications. *Journal of Plant Biochemistry and Biotechnology* 19:9−20

4. Kotake T, Dina S, Konishi T, Kaneko S, Igarashi K, et al. 2005. Molecular cloning of a β-galactosidase from radish that specifically hydrolyzes β-(1→3)- and β-(1→6)-galactosyl residues of arabinogalactan protein. *Plant Physiology* 138:1563−76

5. Smith DL, Abbott JA, Gross KC. 2002. Down-regulation of tomato β-galactosidase 4 results in decreased fruit softening. *Plant Physiology* 129:1755−62

6. de Alcântara PHN, Martim L, Silva CO, Dietrich SMC, Buckeridge MS. 2006. Purification of a β-galactosidase from cotyledons of *Hymenaea courbaril* L. (Leguminosae). Enzyme properties and biological function. *Plant Physiology and Biochemistry* 44:619−27

7. Seddigh S, Darabi M. 2014. Comprehensive analysis of beta-galactosidase protein in plants based on Arabidopsis thaliana. *Turkish Journal of Biology* 38:140−50

8. Tanthanuch W, Chantarangsee M, Maneesan J, Ketudat-Cairns J. 2008. Genomic and expression analysis of glycosyl hydrolase family 35 genes from rice (*Oryza sativa* L.). *BMC Plant Biology* 8:84

9. Fanourakis D, Nikoloudakis N, Paschalidis K, Christopoulos MV, Goumenaki E, et al. 2022. Gene expression, activity and localization of beta-galactosidases during late ripening and postharvest storage of tomato fruit. *Agriculture* 12:778

10. Hou F, Du T, Qin Z, Xu T, Li A, et al. 2021. Genome-wide in silico identification and expression analysis of beta-galactosidase family members in sweetpotato [*Ipomoea batatas* (L.) Lam]. *BMC Genomics* 22:140

11. McCartney L, Ormerod AP, Gidley MJ, Knox JP. 2000. Temporal and spatial regulation of pectic (1→ 4)-*β*-D-galactan in cell walls of developing pea cotyledons: implications for mechanical properties. *The Plant Journal* 22:105−13

12. Sørensen SO, Pauly M, Bush M, Skjøt M, McCann MC, et al. 2000. Pectin engineering: modification of potato pectin by *in vivo* expression of an endo-1,4-*β*-D-galactanase. *Proceedings of the National Academy of Sciences of the United States of America* 97:7639−44

13. Albornos L, Martín I, Pérez P, Marcos R, Dopico B, et al. 2012. Promoter activities of genes encoding *β*-galactosidases from Arabidopsis a1 subfamily. *Plant Physiology and Biochemistry* 60:223−32

14. Moneo-Sánchez M, Izquierdo L, Martín I, Hernández-Nistal J, Albornos L, et al. 2018. Knockout mutants of *Arabidopsis thaliana β*-galactosidase. Modifications in the cell wall saccharides and enzymatic activities. *Biologia Plantarum* 62:80−88

15. Mwaniki MW, Mathooko FM, Matsuzaki M, Hiwasa K, Tateishi A, et al. 2005. Expression characteristics of seven members of the *β*-galactosidase gene family in 'La France' pear (*Pyrus communis* L.) fruit during growth and their regulation by 1-methylcyclopropene during postharvest ripening. *Postharvest Biology and Technology* 36:253−63

16. Esteban R, Labrador E, Dopico B. 2005. A family of *β*-galactosidase cDNAs related to development of vegetative tissue in *Cicer arietinum*. *Plant Science* 168:457−66

17. Sheridan PP, Brenchley JE. 2000. Characterization of a salt-tolerant family 42 *β*-galactosidase from a psychrophilic antarctic *Planococcus* isolate. *Applied and Environmental Microbiology* 66:2438−44

18. Schmid M, Davison TS, Henz SR, Pape UJ, Demar M, et al. 2005. A gene expression map of *Arabidopsis thaliana* development. *Nature Genetics* 37:501−06

19. Sudério FB, Gomes Filho E, Costa JH, Enéas Filho J. 2014. *β*-galactosidases from cowpea stems: properties and gene expression under conditions of salt stress. *Revista Ciência Agronô mica* 45:794−804

20. Spadoni A, Guidarelli M, Sanzani SM, Ippolito A, Mari M. 2014. Influence of hot water treatment on brown rot of peach and rapid fruit response to heat stress. *Postharvest Biology and Technology* 94:66−73

21. Liang W, Chen W, Song R, Zhang F. 2004. Advances in embryo development of longan. *Subtropical Plant Science* 33:65−68

22. Lai Z, Pan L, Chen Z. 1997. Establishment and maintenance of longan embryogenic cell lines. *Journal of Fujian Agricultural University* 26:160−67

23. Qiu X, Feit AS, Feiglin A, Xie Y, Kesten N, et al. 2021. CoBRA: containerized bioinformatics workflow for reproducible ChIP/ATAC-seq Analysis. *Genomics, Proteomics & Bioinformatics* 19:652−61

24. Wang F, Shang G, Wu L, Xu Z, Wang J. 2020. Chromatin accessibility dynamics and a hierarchical transcriptional regulatory network structure for plant somatic embryogenesis. *Developmental Cell* 54:742−757.E8

25. Sijacic P, Bajic M, McKinney EC, Meagher RB, Deal RB. 2018. Changes in chromatin accessibility between Arabidopsis stem cells and mesophyll cells illuminate cell type-specific transcription factor networks. *The Plant Journal* 94:215−31

26. Horstman A, Bemer M, Boutilier K. 2017. A transcriptional view on somatic embryogenesis. *Regeneration* 4:201−16

27. Hoffman BG, Robertson G, Zavaglia B, Beach M, Cullum R, et al. 2010. Locus co-occupancy, nucleosome positioning, and H3K4me1 regulate the functionality of FOXA2-, HNF4A-, and PDX1-bound loci in islets and liver. *Genome Research* 20:1037−51

28. Calo E, Wysocka J. 2013. Modification of enhancer chromatin: what, how, and why? *Molecular Cell* 49:825−37

29. Chen Y, Xie D, Ma X, Xue X, Liu M, et al. 2023. Genome-wide high-throughput chromosome conformation capture analysis reveals hierarchical chromatin interactions during early somatic embryogenesis. *Plant Physiology* 193:555−77

30. Somerville C, Bauer S, Brininstool G, Facette M, Hamann T, et al. 2004. Toward a systems approach to understanding plant cell walls. *Science* 306:2206−11

31. Betekhtin A, Rojek M, Milewska-Hendel A, Gawecki R, Karcz J, et al. 2016. Spatial distribution of selected chemical cell wall components in the embryogenic callus of *Brachypodium distachyon*. *PLoS ONE* 11:e0167426

32. Sala K, Malarz K, Barlow PW, Kurczyńska EU. 2017. Distribution of some pectic and arabinogalactan protein epitopes during *Solanum lycopersicum* (L.) adventitious root development. *BMC Plant Biology* 17:25

33. Sampedro J, Gianzo C, Iglesias N, Guitián E, Revilla G, et al. 2012. AtBGAL10 is the main xyloglucan *β*-galactosidase in Arabidopsis, and its absence results in unusual xyloglucan subunits and growth defects. *Plant Physiology* 158:1146−57

34. Prakash A, Jeffryes M, Bateman A, Finn RD. 2017. The HMMER web server for protein sequence similarity search. *Current Protocols in Bioinformatics* 60:3.15.1−3.15.23

35. Kumar S, Stecher G, Li M, Knyaz C, Tamura K. 2018. MEGA X: molecular evolutionary genetics analysis across computing platforms. *Molecular Biology and Evolution* 35:1547−49

36. Wang Y, Li J, Paterson AH. 2013. *MCScanX*-transposed: detecting transposed gene duplications based on multiple colinearity scans. *Bioinformatics* 29:1458−60

37. Chen C, Chen H, Zhang Y, Thomas HR, Frank MH, et al. 2020. TBtools: an integrative toolkit developed for interactive analyses of big biological data. *Molecular Plant* 13:1194−202

38. Meng D, Yang Q, Dong B, Song Z, Niu L, et al. 2019. Development of an efficient root transgenic system for pigeon pea and its application to other important economically plants. *Plant Biotechnology Journal* 17:1804−13

39. Yang X, Zhang X, Fu L, Min L, Liu G. 2010. Multiple shoots induction in wild cotton (*Gossypium bickii*) through organogenesis and the analysis of genetic homogeneity of the regenerated plants. *Biologia* 65:496−503

40. Livak KJ, Schmittgen TD. 2001. Analysis of relative gene expression data using real-time quantitative PCR and the $2^{-\Delta\Delta C_T}$ method. *Methods* 25:402−08

41. Lin Y, Min J, Lai R, Wu Z, Chen Y, et al. 2017. Genome-wide sequencing of longan (*Dimocarpus longan* Lour.) provides insights into molecular basis of its polyphenol-rich characteristics. *GigaScience* 6:gix023

42. Yamaguchi-Shinozaki K, Shinozaki K. 2005. Organization of *cis*-acting regulatory elements in osmotic- and cold-stress-responsive promoters. *Trends in Plant Science* 10:88−94

43. Latchman DS. 1993. Transcription factors: an overview. *International Journal of Experimental Pathology* 74:417−22

44. Spitz F, Furlong EEM. 2012. Transcription factors: from enhancer binding to developmental control. *Nature Reviews Genetics* 13:613−26

45. Bae S, Lesch BJ. 2020. H3K4me1 distribution predicts transcription state and poising at promoters. *Frontiers in Cell and Developmental Biology* 8:289

46. Guo S, Song J, Zhang B, Jiang H, Ma R, et al. 2018. Genome-wide identification and expression analysis of beta-galactosidase family members during fruit softening of peach [*Prunus persica* (L.) Batsch]. *Postharvest Biology and Technology* 136:111−23

47. Othman R, Chong HL, Choo TS, Ali ZM. 2011. Three *β*-galactosidase cDNA clones related to fruit ripening in papaya (*Carica papaya*). *Acta Physiologiae Plantarum* 33:2301−10

48. Chandrasekar B, van der Hoorn RAL. 2016. Beta galactosidases in Arabidopsis and tomato-a mini review. *Biochemical Society Transactions* 44:150−58

49. Hobson N, Deyholos MK. 2013. Genomic and expression analysis of the flax (*Linum usitatissimum*) family of glycosyl hydrolase 35 genes. *BMC Genomics* 14:344

50. Du L, Tang Z, Wu X, Chen C, Lai B. 2023. Genome-wide identification and expression analysis of *β*-galactosidase family members in *Brassica juncea* var. *tumida*. *Molecular Plant Breeding* 21:472−86

51. Barnes WJ, Anderson CT. 2018. Release, recycle, rebuild: cell-wall remodeling, autodegradation, and sugar salvage for new wall biosynthesis during plant development. *Molecular Plant* 11:31−46

52. Mohnen D. 2008. Pectin structure and biosynthesis. *Current Opinion in Plant Biology* 11:266−77

53. Palin R, Geitmann A. 2012. The role of pectin in plant morphogenesis. *Biosystems* 109:397−402

54. Van Hengel AJ, Van Kammen A, De Vries SC. 2002. A relationship between seed development, Arabinogalactan-proteins (AGPs) and the AGP mediated promotion of somatic embryogenesis. *Physiologia Plantarum* 114:637−44

55. Rodríguez-Sanz H, Manzanera JA, Solís MT, Gómez-Garay A, Pintos B, et al. 2014. Early markers are present in both embryogenesis pathways from microspores and immature zygotic embryos in cork oak, *Quercus suber* L. *BMC Plant Biology* 14:224

56. Liu ZJ, Wu S, Junwen Z. 2020. A review of MADS-box genes, the molecular regulatory genes for floral organ development in Orchidaceae. *Acta Horticulturae Sinica* 47:2047−62

57. Thakare D, Tang W, Hill K, Perry SE. 2008. The MADS-domain transcriptional regulator AGAMOUS-LIKE15 promotes somatic embryo development in Arabidopsis and soybean. *Plant Physiology* 146:1663−72

58. Ban Q, Ye H, He Y, Jin M, Han S, et al. 2018. Functional characterization of persimmon *β*-galactosidase gene *DkGAL1* in tomato reveals cell wall modification related to fruit ripening and radicle elongation. *Plant Science* 274:109−20

59. Lazan H, Ng SY, Goh LY, Ali ZM. 2004. Papaya *β*-galactosidase/galactanase isoforms in differential cell wall hydrolysis and fruit softening during ripening. *Plant Physiology and Biochemistry* 42:847−53

60. Dean GH, Zheng H, Tewari J, Huang J, Young DS, et al. 2007. The *Arabidopsis MUM2* gene encodes a *β*-galactosidase required for the production of seed coat mucilage with correct hydration properties. *The Plant Cell* 19:4007−21

61. Gantulga D, Turan Y, Bevan DR, Esen A. 2008. The *Arabidopsis* At1g45130 and At3g52840 genes encode beta-galactosidases with activity toward cell wall polysaccharides. *Phytochemistry* 69:1661−70

62. Wei H, Brunecky R, Donohoe BS, Ding SY, Ciesielski PN, et al. 2015. Identifying the ionically bound cell wall and intracellular glycoside hydrolases in late growth stage *Arabidopsis stems*: implications for the genetic engineering of bioenergy crops. *Frontiers in Plant Science* 6:315

63. Gantulga D, Ahn YO, Zhou C, Battogtokh D, Bevan DR, et al. 2009. Comparative characterization of the *Arabidopsis* subfamily a1 *β*-galactosidases. *Phytochemistry* 70:1999−2009

64. Yu L, Miao Z, Qi G, Wu J, Cai X, et al. 2014. MADS-box transcription factor AGL21 regulates lateral root development and responds to multiple external and physiological signals. *Molecular Plant* 7:1653−69

65. Du J, Anderson CT, Xiao C. 2022. Dynamics of pectic homogalacturonan in cellular morphogenesis and adhesion, wall integrity sensing and plant development. *Nature Plants* 8:332−40

66. Du J, Kirui A, Huang S, Wang L, Barnes WJ, et al. 2020. Mutations in the pectin methyltransferase QUASIMODO2 influence cellulose biosynthesis and wall integrity in Arabidopsis. *The Plant Cell* 32:3576−97

67. Shekhawat K, Almeida-Trapp M, García-Ramírez GX, Hirt H. 2022. Beat the heat: plant- and microbe-mediated strategies for crop thermotolerance. *Trends in Plant Science* 27:802−13

68. Zhang S, Zhu C, Zhang X, Liu M, Xue X, et al. 2023. Single-cell RNA sequencing analysis of the embryogenic callus clarifies the spatiotemporal developmental trajectories of the early somatic embryo in *Dimocarpus longan*. *The Plant Journal* 115:1277−97

69. Yao C. 2019. *Expression, enzymatic properties and stabilization of cold-adapted β-galactosidase from deep-sea microorganism*. Thesis. Shanghai: Shanghai Ocean University.

70. Bi A, Wang T, Wang G, Zhang L, Wassie M, et al. 2022. Corrigendum for: stress memory gene *FaHSP17.8-CII* controls thermotolerance via remodeling PSII and ROS signaling in tall fescue. *Plant Physiology* 188:670

71. Ashraf M, Harris PJC. 2005. *Abiotic stresses: plant resistance through breeding and molecular approaches*. Boca Raton: CRC Press. 766 pp. https://doi.org/10.1201/9781482293609

72. Yang B, Chen Y, Shi J. 2019. Reactive oxygen species (ROS)-based nanomedicine. *Chemical Reviews* 119:4881−985